

Astro-Det: Resident Space Object Detection for Space Situational Awareness

Yuhang Zhang[†], Rangya Zhang[†], Qianlei Jia, Jiaping Xiao, Lu Bai, and Mir Feroskhan*

School of Mechanical and Aerospace Engineering, Nanyang Technological University
{yuhang004, rangya001, jiaping001}@e.ntu.edu.sg, {qianlei.jia, bailu, mir.feroskhan}@ntu.edu.sg

Abstract—The flourishing space industry has caused a significant increase in space debris, posing a critical risk to high-asset operational spacecraft. A particular challenge is identifying small-sized debris characterized by low reflectivity and rapid motion. Traditional ground-based detection methods, constrained by geographic and daylight limitations, necessitate an exploration of in-space debris identification to bolster spacecraft's space situational awareness (SSA) capability. Onboard optical sensors, which generate high-resolution images, offer crucial data for these tasks. Considering the sparsity and low signal-to-noise ratio (SNR) in space scenario images, this paper introduces an Astro-Det framework to detect streaks and aggregated spots in sparse environments. Within this framework, morphological and learning-based methodologies are independently applied to assess the effectiveness of object detection in space. A novel onboard camera-based space dataset is leveraged to evaluate the framework. Simulation results reveal that while the morphological approach falls short in detection accuracy compared to the learning-based approach, it demonstrates superior computational efficiency. This research presents detailed comparative evaluation, providing valuable insights into how these established algorithms perform under the unique conditions of sparse space scenarios.

Index Terms—sparse object detection, onboard camera, morphological analysis, deep learning

I. INTRODUCTION

In recent decades, the expansion of the space industry has led to a significant increase in the number of Resident Space Objects (RSOs) in Near-Earth Orbit (NEO). Since 1957, over 20,000 objects, each larger than 10 cm in diameter, have been tracked [1]. Among these, only about 1,000 are operational satellites, while the vast majority are space debris resulting from collisions and decommissioned spacecraft. Notably, RSOs larger than one centimeter pose serious risks to any spacecraft in NEO [2, 3]. Therefore, the development of Space Situational Awareness (SSA) capabilities for detecting and predicting the positions of RSOs is important.

To date, SSA systems are primarily categorized into ground-based and space-based systems. Ground-based SSA systems rely mainly on phased array radars and optical telescopes, but are subject to geographical and sunlight limitations, which can restrict their applications [4, 5]. In contrast, space-based SSA

systems, which utilize onboard optical devices like cameras, are not constrained by these limitations [6]. Cameras are cost-effective and lightweight, enabling long-term sensory data collection without significantly increasing the payload of spacecraft. Consequently, the use of cameras for object detection is obtaining increasing attention, highlighting their potential in the field of space safety and debris monitoring.

However, the space environment, characterized by both its vastness and predominantly black expanse, presents unique challenges in image analysis. This complex aspect leads to optical cameras often capturing predominantly low SNR grayscale images. Furthermore, due to the observed trailing phenomenon, targets often appear as streak-like shapes in these images. These distinct characteristics classify the detection of targets in space as a form of small target detection within sparsely annotated datasets. Current research in this fascinating field can be broadly categorized into two methodologies: non-learning based methods and learning-based methods.

1) *Non-learning based methods*: Although there is a rich variety of non-learning based object detection methods available, the unique trailing phenomenon in RSO detection makes morphology-based methods particularly well-suited for this task. For instance, a novel approach for detecting streak-like targets in single optical images was introduced in [7]. The multi-target detection technique proposed in [8] utilized topological scanning, addressing the limitations of traditional methods that require longer sequences or accurate initialization. Yao et al. [9] presented an adaptive space objects detection algorithm, effectively suppressing background noise and distortion, thus enabling rapid detection of space targets. Furthermore, Zou et al. [10] applied local grayscale correlation between two image frames for space target search and positioning, circumventing the issue of false target verification inherent in traditional blind detection. These analyses indicate that morphology-based detection methods are increasingly being applied to RSO detection, demonstrating their efficacy and adaptability in this specialized context.

2) *Learning based methods*: The application of learning-based methods for RSO detection can enhance the adaptability and efficiency of the detection process. However, as far as our knowledge extends, the current body of research in this domain remains relatively limited. Scholars have, thus far, only proposed a real-time dim space target detection algorithm utilizing convolutional neural networks and attention modules in [11]. Despite this, learning-based object detection algorithms have

This work was supported by the Economic Development Board (EDB) under its Space Technology Development Programme (STDP) Thematic Grant Call on Space Technologies (Award S23-020019-STDP). ([†] Yuhang Zhang and Rangya Zhang are co-first authors.) (*Corresponding author: Mir Feroskhan.)

Y. Zhang, R. Zhang, Q. Jia, J. Xiao, L. Bai and M. Feroskhan are with the School of Mechanical and Aerospace Engineering, Nanyang Technological University, Singapore 639798, Singapore.

proven effective and found extensive applications in various fields [12]. Therefore, there is a need for increased attention to the development of learning-based object detection algorithms specifically tailored for RSO monitoring.

In this study, an Astro-Det framework is explicitly designed to effectively tackle the challenge of detecting sparsely distributed targets in the camera-based space scenario. This framework comprises two distinct modules: the morphological detection module, which differentiates various targets by identifying their geometric discrepancies, and the learning-based detection module, which distinguishes targets by minimizing the difference between predicted values and ground truth. Furthermore, we use a novel dataset to validate the efficacy of the proposed framework. It stands distinct from conventional object detection datasets by presenting unique challenges: the vast and feature-sparse nature of space scenarios, subtle variances in observable features, and the high degree of freedom in camera movement. A comparative analysis is performed based on this dataset to evaluate the performance of the two modules comprehensively. To the best of our knowledge, this represents a novel endeavor to deploy traditional and learning-based approaches within a vision-based space surveillance environment, offering a novel insight for the further development and selection of sparse object detection algorithms.

The rest of the paper is organized as follows. Section II introduces the proposed methodology, including the data acquisition procedure and the proposed Morphology-based and learning-based methods. Simulation results and detailed analysis are presented in Section III. Finally, Section IV gives the conclusion.

II. METHODOLOGY

In this study, a dataset was acquired and generated within a simulated environment for the object detection task. The dataset comprises over 2000 high-resolution, 16-bit depth TIFF images (4418×4418 pixels). It also provides detailed camera specifications, the target's catalog ID, and the bearing angle with the tracker as ground truth. Subsequently, a module incorporating both morphology-based and learning-based algorithms was developed to address the problem of sparse object identification in space environments. Fig. 1 presents the comprehensive framework of the dataset acquisition and the strategic application of algorithms. The related details are further discussed in the subsequent sections.

A. Data Acquisition

The data acquisition procedure employed in this expanded study simulates authentic camera parameters and space object orbits. Initially, the simulation propagated the orbits of approximately 25,000 celestial objects using Two-Line Element sets (TLEs) [13] within a predetermined time frame as depicted in the simulation segment of Fig. 1. In parallel, a tracker's orbit was consistently defined and propagated, ensuring alignment with the observational framework.

Furthermore, camera specifications were leveraged to determine its sensitivity, a pivotal factor for precise detection.

The simulation then proceeded to identify objects crossing the camera's field of view by applying the tracker's position and camera pointing directions at each simulation step. Notably, three field-of-view intersecting cameras were employed to expand the overall perceptual range. Objects visible to the camera were further filtered based on detailed sensitivity analyses. As the camera's FPS was set to 1, the target's bearing angle and catalog ID were recorded over a one-second interval. These details, combined with the camera's focal length, enabled the calculation of the target's precise coordinates within the imaging coordinate system of the tracker. This information serves as the ground truth for the bounding box in the object detection task.

Images were generated for each timestamp, creating streaks or spots that represent the objects, calculated with exact pixel values and point spread functions for both the background stars and object streaks. Concurrently, reference images were produced, with streaks and spots clearly marked with their associated catalog IDs. Raw images simulate grayscale photographs captured by cameras in a real-space environment. Reference images, on the other hand, are processed versions of raw images for better visualization of the images and target features. Examples of reference images from different datasets are showcased in Fig. 2. Due to the tracker's position and camera pointing directions, during the simulated time interval, Cam1 exhibits a high density of spot targets, Cam2 shows an intermediate distribution of streaks and spots, and Cam3 primarily captures streak targets.

B. Astro-Det

Astro-Det is a framework that includes two distinct units, morphological and learning-based, capable of independently performing sparse target detection tasks. The following section provides a detailed description of the structures and principles of these two modules.

1) *Morphology-Based Sparse Object Detection*: Given that the dataset comprises a significantly higher proportion of noise than targets in this study, the Astro-Det architecture introduces a morphology-based target detection module considering the substantial geometric disparity between targets and noise. This module is adept at identifying streaks and aggregated spots from sparse environments. The process begins with binarizing the input image, effectively eliminating noise characterized by lower brightness levels:

$$B(x, y) = \begin{cases} 255 & \text{if } I(x, y) \geq k\mu \\ 0 & \text{otherwise} \end{cases}, \quad (1)$$

where $B(x, y)$ is the pixel value of the binarized image at position (x, y) , $I(x, y)$ is the pixel value of the original image at (x, y) , μ denotes the average pixel value of the image, and k is an empirical constant. Thus, the 16-bit input image is converted into an 8-bit binary grayscale image.

Subsequently, each obtained subsection undergoes a morphological closing operation leveraging a structuring element S . This step is designed to fill in the gaps between discrete

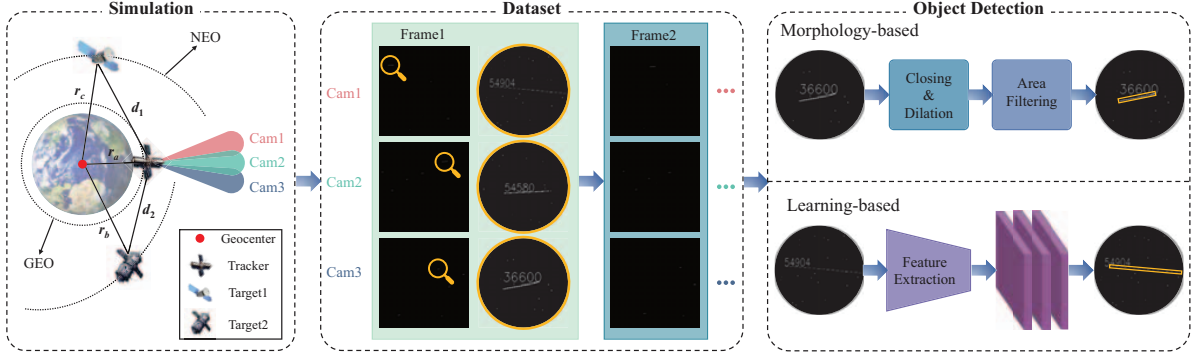


Fig. 1. Workflow for sparse target detection: (1) Schematic representation of the simulation process; (2) Dataset generation procedure; (3) Structural framework of Astro-Det, progressing from left to right.

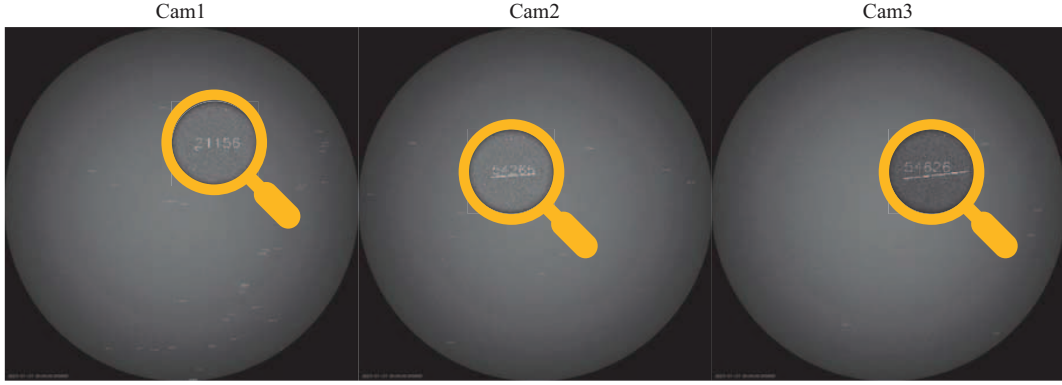


Fig. 2. Examples of images from different datasets. (1) An image case in Cam1. The most targets, with targets predominantly of “spot” shapes. (2) An image case in Cam2. A relatively balanced mix of targets with “spot” and “streak” shapes. (3) An image case in Cam3. The fewest targets, with targets mostly of “streak” shapes.

streaks and eliminate noise in the decontaminated image, resulting in a more refined processed image:

$$P = (B \oplus S) \ominus S, \quad (2)$$

where S is the structuring element, \oplus denotes the dilation operation, and \ominus signifies the erosion operation. Dilation and erosion operations are each defined as follows:

$$\begin{aligned} (B \oplus S)(x, y) &= \max_{(s_x, s_y) \in S} B(x + s_x, y + s_y) \\ (B \ominus S)(x, y) &= \min_{(s_x, s_y) \in S} B(x + s_x, y + s_y), \end{aligned} \quad (3)$$

where (s_x, s_y) represents the coordinates in S .

These processed images are then subjected to area thresholding. In this phase, any connected region with an area exceeding the predefined threshold is preserved. Finally, the coordinates of the upper-left and lower-right corners of all retained areas are accurately determined for the filtered images. These coordinates are leveraged to define the bounding boxes around these areas. The detailed workflow is presented in Algorithm 1.

2) Learning-Based Sparse Object Detection: In light of the large image sizes, data preprocessing is employed in the proposed Astro-Det architecture before training process of the learning-based method. The methodology commences by splitting the dataset into training, validation, and test subsets in a 7: 2: 1 ratio, applying the holdout method to aid in the model’s evaluation process.

To address the issue of large image dimensions, the images are initially segmented into smaller sections measuring 260×260 pixels each. This segmentation process includes a twenty percent overlap in both horizontal and vertical directions, serving as a strategy for data augmentation. Additionally, the annotations of the labels are accurately adjusted to match the newly segmented dimensions. Given the inherent sparse labeling of the dataset, 96% of the segmented images do not contain the target. Addressing the risk of overfitting caused by a high proportion of negative samples (images without targets), the training dataset is selectively pruned to remove a substantial number of negative samples. This strategy is directed towards creating a more balanced dataset, aiming

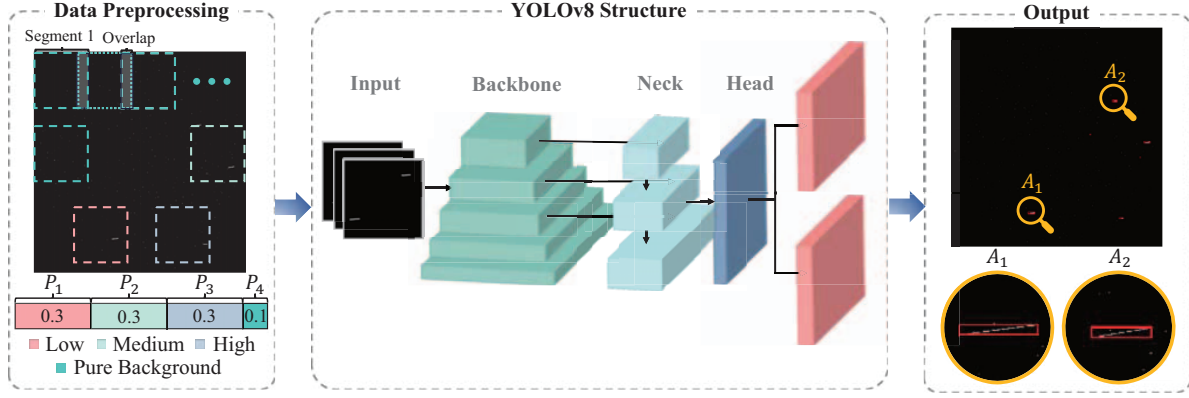


Fig. 3. Workflow for learning-based detection method: (1) data preprocessing. The proportions P_1 to P_4 denote the segmentation of segmented images labeled as low, medium, high, and pure background respectively after data balancing; (2) YOLOv8 structure [14]; (3) prediction results of learning-based method. A_1 and A_2 represent localized zoomed-in images.

Algorithm 1 Morphology-Based Sparse Object Detection

Input:

I : Input raw image

Output:

$C = \{C_1, C_2, \dots, C_n\}$, where C_t represents the coordinates of the t -th bounding box

- 1: Binarize I to obtain B
- 2: **for** each position (x, y) in B **do**
- 3: Create a subsection image $B(x + s_x, y + s_y)$
- 4: Perform closing operation on the subsection image
- 5: Calculate the area A_s of the closed subsection
- 6: **if** $A_s \geq A_T$, where A_T is the area threshold **then**
- 7: Define bounding box $C_t = (x_{\min}, y_{\min}, x_{\max}, y_{\max})$
- 8: Add C_t to a temporary list T
- 9: **end if**
- 10: **end for**
- 11: Initialize list C for merged bounding boxes
- 12: **for** each pair (C_i, C_j) in T **do**
- 13: Calculate IOU: $\text{IOU}(C_i, C_j) = \frac{\text{area}(C_i \cap C_j)}{\text{area}(C_i \cup C_j)}$
- 14: **if** $\text{IOU}(C_i, C_j) \geq \text{IOU_Threshold}$ **then**
- 15: Merge C_i and C_j into C_n
- 16: Add C_n to list C
- 17: **end if**
- 18: **end for**
- 19: **return** C

for an approximate 0.9:0.1 ratio between images with and without targets. For the validation and test datasets, selective pruning is omitted to maintain the accuracy and validity of model evaluation. Furthermore, the dataset is enhanced by introducing three labels: “low”, “medium”, and “high”, based on the target-tracker proximity. This augmentation counters potential issues of poor generalization and low accuracy associated with a single label like ‘target’, ensuring an even distribution among these new categories. Considering the small

size of most targets, images are resized to 640×640 pixels to enhance target features.

Following the completion of the data preprocessing steps, the learning model is then employed for training and validation on the processed dataset. The workflow for learning-based detection method is shown in Fig. 3. In the domain of learning-based RSO detection, YOLOv8 [14] is selected for its established efficacy in object detection tasks. YOLOv8 is distinguished by its rapid processing capabilities, high accuracy, and enhanced proficiency in detecting objects [15, 16], which aligns well with the requirements of RSO imagery analysis. Upon completion of the training phase, the model exhibiting the best performance on the validation dataset is subsequently selected for prediction on the test dataset.

III. SIMULATION RESULTS AND ANALYSIS

In this section, we evaluate the proposed morphology-based and learning-based sparse object detection methods on the simulated datasets. Both qualitative and quantitative results are presented, as depicted in Fig. 4 and Table I, respectively.

A. Morphology Performance Analysis

To better visualize the result in Fig. 4, areas containing targets with more distinctive features are locally enlarged to demonstrate the effectiveness of the proposed approach. For the morphological approach, it can be seen that streaks are detected effectively in these areas, but false and missed detections occur for aggregated spots of smaller sizes. This phenomenon may be principally attributed to the noise distribution in the image. Specifically, in regions with dense noise, the dilation process of the closing operation might have connected separate spots. Conversely, in sparsely noisy regions containing target spots, the erosion process of the closing operation might have made smaller spots less distinct, thus leading to false and missed detection issues.

Moreover, Table I employs several indicators to further elucidate the performance of the proposed algorithms. Notably,

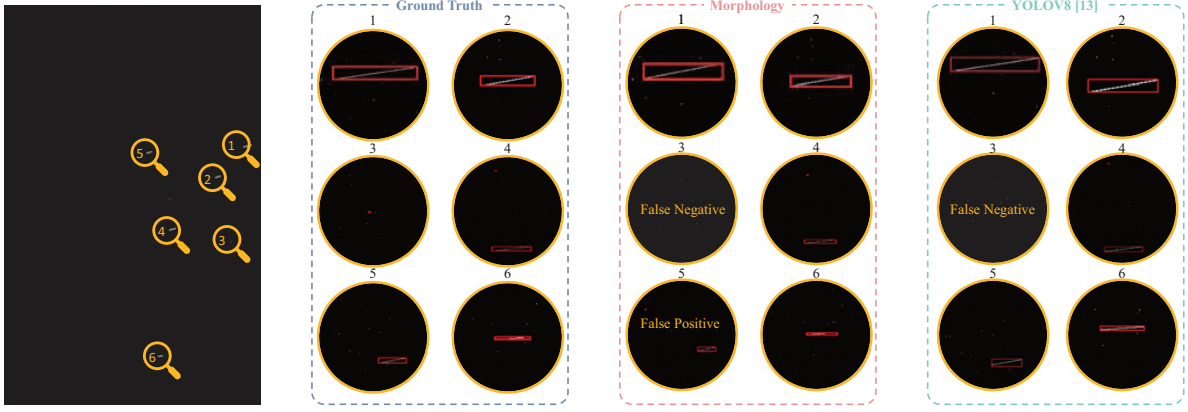


Fig. 4. Object detection results. Several selected regions are locally enlarged to illustrate the model's performance.

TABLE I
COMPARATIVE PERFORMANCE METRICS OF MORPHOLOGICAL AND LEARNING-BASED APPROACHES

Method	Dataset	Total		Predict	Precision	Recall	F1 Score	SNR	Detect Time / Img (s)
		GT	Predict	Right					
Morphological	Cam1	4686	1016	682	0.67	0.15	0.24	0.72	0.40
	Cam2	888	701	370	0.53	0.42	0.47	0.63	0.21
	Cam3	462	692	315	0.46	0.68	0.55	0.55	0.20
Learning-Based	Cam1	1541	1329	1254	0.94	0.81	0.87	0.72	1.06
	Cam2	153	129	124	0.96	0.81	0.88	0.63	1.07
	Cam3	180	124	107	0.86	0.59	0.70	0.55	1.09

Cam1 is characterized by a high density of spot targets, while Cam3 predominantly contains streak targets. The distribution of streaks and spots in Cam2 is intermediate. It is evident that the morphological algorithm demonstrates the best overall performance in Cam3, with both precision and recall being relatively high. This superior performance can be attributed to the predominance of streak targets in Cam3, which are significantly more distinct from the noise geometry, resulting in relatively minimal false and missed detections. However, the performance on Cam1 is not as satisfactory. Despite achieving the highest precision among the three datasets, its recall is considerably lower. This suboptimal performance in Cam1 stems from the abundance of small spot targets, which present a significant challenge to the morphological algorithm, leading to a notable proportion of missed detections.

B. YOLO Performance Analysis

The application of the YOLOv8 model demonstrates high accuracy in detecting targets, as evidenced by the comparison between the detection results and ground truth illustrated in Fig. 4. The model efficiently identifies targets with distinct streak-like features and also successfully detects some smaller, dot-like targets. However, it occasionally exhibits false positives in areas lacking clear characteristics. This should be attributed to the model's sensitivity to subtle variations in the image, where it sometimes misinterprets noise or less defined

regions as targets. This model's advanced pattern recognition capabilities, while adept at capturing evident features, can lead to over-detection in areas where target characteristics are not pronounced.

As detailed in Table I, for Cam1, despite containing numerous spot targets that are challenging to discern with the human eye, the model performs effectively due to the abundance of learnable targets and the higher average brightness of these spot targets. In Cam2, the distribution of features from different target types is more balanced, resulting in better detection outcomes. However, in Cam3, despite a higher prevalence of streak targets, the model encounters more false positives leading to a lower recall number. This is attributed to the lower brightness of streak targets, making their luminance features less distinct.

C. Comparative Analysis

The comparative analysis depicted in Table I reveals a trade-off between the morphological and learning-based approaches. While the learning-based method, exemplified by YOLOv8 [14], demonstrates superior accuracy in target detection in space environment, it falls behind in terms of processing speed, averaging about 1 second per image. Conversely, the morphological approach, though less effective in detection precision, excels in computational efficiency, completing processing in approximately 0.2 seconds per image.

This contrast underscores the practical implications of choosing between these methods based on specific operational needs. The morphological approach, with its faster processing rate, is particularly advantageous in scenarios where real-time data processing is critical, such as in live tracking or immediate threat detection in space environments. On the other hand, the learning-based method's superior accuracy makes it ideal for applications where the precision of target identification is paramount, such as in detailed space surveillance and research-oriented tasks where every potential target needs to be accurately cataloged. Thus, the selection between these methods can be strategically aligned with the specific objectives and constraints of various space missions.

IV. CONCLUSION

This study explores the challenge of sparse object detection in space environments. The Astro-Det framework, which integrates morphological and learning modules, is proposed to identify different targets in space. A dataset derived from a simulated environment is leveraged to evaluate the algorithm's performance. The results demonstrate that the accuracy of the morphological approach, which is a non-date-driven approach relying on the geometric attributes of objects, is inferior to the learning-based approach and shows relatively limited generalizability. Nevertheless, despite its limited efficacy, morphological algorithms can be applied directly and exhibit superior computational efficiency. In contrast, the learning-based algorithm necessitates a substantial amount of labeled ground truth data to guarantee higher accuracy and robustness at the expense of slower computational performance.

On the basis of these findings, future work will aim to integrate morphological and learning-based algorithms. The low SNR of space datasets presents a considerable challenge for the feature extraction component of the learning-based algorithm. Inspired by the capability of morphological methods to extract geometric features of various objects effectively, it is reasonable to embed these geometric insights into the feature extraction module of the learning-based algorithm. This combination is anticipated to enhance the algorithm's speed and accuracy simultaneously. Furthermore, the object tracking algorithm will also be advanced to establish a robust and real-time RSO inspection and tracking system to better adapt to space's uncertain and dynamic nature.

REFERENCES

- [1] J. A. Kennewell and B.-N. Vo, "An overview of space situational awareness," in *Proceedings of the 16th International Conference on Information Fusion*. IEEE, 2013, pp. 1029–1036.
- [2] W. Flury, A. Massart, T. Tchildknecht, U. Hugentobler, J. Kuusela, and Z. Sodnik, "Searching for small debris in the geostationary ring," *ESA bulletin*, vol. 104, no. November, pp. 92–100, 2000.
- [3] N. L. Johnson, "Orbital debris: the growing threat to space operations," in *33rd Annual Guidance and Control Conference*, no. AAS 10-011, 2010.
- [4] B. Weeden, P. Cefola, and J. Sankaran, "Global space situational awareness sensors," in *AMOS Conference*, 2010.
- [5] A. Munir, A. Aved, and E. Blasch, "Situational awareness: techniques, challenges, and prospects," *AI*, vol. 3, no. 1, pp. 55–77, 2022.
- [6] B. Lal, A. Balakrishnan, B. M. Caldwell, R. S. Buenconsejo, and S. A. Carioscia, "Global trends in space situational awareness (ssa) and space traffic management (stm)," *Science and Technology Policy Institute*, vol. 10, 2018.
- [7] B. Lin, L. Zhong, S. Zhuge, X. Yang, Y. Yang, K. Wang, and X. Zhang, "A new pattern for detection of streak-like space target from single optical images," *IEEE Transactions on Geoscience and Remote Sensing*, vol. 60, pp. 1–13, 2021.
- [8] B. Lin, X. Yang, J. Wang, Y. Wang, K. Wang, and X. Zhang, "A robust space target detection algorithm based on target characteristics," *IEEE Geoscience and Remote Sensing Letters*, vol. 19, pp. 1–5, 2021.
- [9] Y. Yao, J. Zhu, Q. Liu, Y. Lu, and X. Xu, "An adaptive space target detection algorithm," *IEEE Geoscience and Remote Sensing Letters*, vol. 19, pp. 1–5, 2022.
- [10] Y. Zou, J. Zhao, Y. Wu, B. Wang, and L. Dong, "Reverse procedure detection of space target streaks based on motion parameter estimation," *IEEE Access*, vol. 9, pp. 21 823–21 831, 2021.
- [11] X. Guo, T. Chen, J. Liu, Y. Liu, and Q. An, "Dim space target detection via convolutional neural network in single optical image," *IEEE Access*, vol. 10, pp. 52 306–52 318, 2022.
- [12] J. Xiao, J. H. Chee, and M. Feroskhan, "Real-time multi-drone detection and tracking for pursuit-evasion with parameter search," *IEEE Transactions on Intelligent Vehicles*, 2024.
- [13] C. Levit and W. Marshall, "Improved orbit predictions using two-line elements," *Advances in Space Research*, vol. 47, no. 7, pp. 1107–1115, 2011.
- [14] G. Jocher, A. Chaurasia, and J. Qiu, "YOLO by Ultralytics," Jan. 2023. [Online]. Available: <https://github.com/ultralytics/ultralytics>
- [15] A. Vats and D. C. Anastasiu, "Enhancing retail checkout through video inpainting, yolov8 detection, and deepsort tracking," in *Proceedings of the IEEE/CVF Conference on Computer Vision and Pattern Recognition*, 2023, pp. 5529–5536.
- [16] A. Aboah, B. Wang, U. Bagci, and Y. Adu-Gyamfi, "Real-time multi-class helmet violation detection using few-shot data sampling technique and yolov8," in *Proceedings of the IEEE/CVF Conference on Computer Vision and Pattern Recognition*, 2023, pp. 5349–5357.